Accidental Releases of Hydrogen in Maintenance Garages: Modelling and Assessment

A. John, R. David, Z. Liang
Canadian Nuclear Laboratories, Chalk River, Ontario, Canada
aneesh.john@cnl.ca, robert.david@cnl.ca, zheliang@cnl.ca

ABSTRACT

This study investigates the light gas dispersion behaviour in a maintenance garage with natural or forced ventilation. A scaled-down garage model (0.71 m high, 3.07 m long and 3.36 m wide) equipped with gas and velocity sensors was used in the experiments. The enclosure had four rectangular vents at the ceiling and four at the bottom on two opposing side walls. The experiments were performed by injecting helium continuously through a 1-mm downward-facing nozzle until a steady state was reached. The sensitivity parameters included helium injection rate, the elevation of the injection nozzle and forced flow speeds. Exhaust fans were placed at one or all of the top vent(s) to mimic forced ventilation. Numerical simulations conducted using GOTHIC, a general-purpose thermal-hydraulic code, and calculations with engineering models were compared with experimental measurements to determine the relative suitability of each approach to predict the light gas transport behaviour. The GOTHIC simulations captured the trends of the helium distribution, gas movement in the enclosure, and the passive vent flows reasonably well. Lowesmith's model predictions for the helium transients in the upper uniform layer were also in good agreement with the natural venting experiments.

1.0 INTRODUCTION

Hydrogen is becoming one of the potential replacements for fossil fuel-based vehicles (light-, medium- or heavy-duty) due to the increasing pressure for low-carbon and low-emission transportation. The rapid growth in the use of hydrogen for transportation sectors will create a demand for suitable maintenance facilities and parking garages. Design or retrofitting of these facilities must ensure that they are safe in the event of unintended hydrogen releases [1]. Hydrogen leaks are a significant safety concern in confined spaces as they can accumulate, resulting in fire and explosion hazards. Adequate ventilation or appropriate mitigation measures are required to prevent such events from occurring.

The accumulation of hydrogen (or helium, a surrogate gas of hydrogen) in indoor facilities or enclosures has been studied experimentally and numerically by many researchers. Gupta et al. [2] evaluated the helium dispersion and mixing characteristics in a 41 m^3 unobstructed enclosure without ventilation. The analysis showed that the risk incurred is most strongly affected by the total volume of gas released rather than the flow rate. Cariteau et al. [3] studied the helium build-up using the same 41 m^3 enclosure with or without a vent at release rates ranging from 0.1 to 18 SLPM (standard litres per minute). They found with small distributed leaks or a vent opening at the floor or ceiling, vertical stratification of helium was developed and the concentration difference became larger at higher release rates. Houssin-Agbomson et al. [4] examined the effects of wind speed on helium dispersion in a 1 m^3 enclosure with one or two vents at release rates varying from 1 to 100 SLPM. The study showed that wind could positively or negatively impact the helium build-up depending on the wind speed and direction. Liang et al. [5] [6] examined the helium dispersion behaviour in a 16.6 m^3 enclosure with distributed leaks along the edges or vents of varying sizes with buoyancy-driven natural ventilation or forced flow at the vent. After a continuous release of helium, the vertical helium profile always reached a steady state, consisting of a homogenous layer at the top and a stratified layer at the bottom. The helium transients in the upper uniform layer were well predicted by the models developed by Lowesmith et al. [7] and Prasad and Yang [8].

Choi et al. [9] investigated the effectiveness of ventilation to mitigate the accumulation of hydrogen gas in a parking garage (16.7 m × 18.0 m × 2.3 m). Their simulations showed that the majority of the hydrogen leaked from the bottom of a car moved up and flowed parallel to the ceiling, and the hydrogen concentration near the ceiling was relatively uniform in space. Ehrhart et al. [1] performed a hazard and

operability study to identify risk-significant scenarios related to light-duty hydrogen vehicles in a repair garage (24.4 m × 25.6 m × 4.8 m). Their simulations showed that the position, direction, and velocity of ventilation have a significant impact on the amount of instantaneous flammable mass accumulated below the car. Chen et al. [10] examined the near- and far-field helium dispersion behaviour in a scale-down garage model (1.5 m × 2.5 m × 0.24 m). They also demonstrated that the gas plume driven by the buoyancy reached the ceiling and spread in all directions resulting in a flammable layer across the ceiling. Xin et al. [11] also conducted helium experiments in a reduced-scale garage (3.3 m × 3.9 m × 0.5 m) and found that the initial release rate was the main factor in determining gas concentration distribution. They observed that the structural beams in the garage affected the distribution since helium fills the spaces between beams until it reaches the height of the beam before spilling over to other sections of the garage. Huang et al. [12] carried out numerical modelling of hydrogen distribution in a underground parking garage (60 m × 36 m × 5.8 m). They found that a flammable cloud of hydrogen only developed at the bottom and sides of the car. They also found that vents located in the garage ceiling corners provided better hydrogen removal, and car position, relative to the side wall in the garage, did not significantly affect the horizontal dispersion speed.

The helium dispersion experiments performed in a 16.6 m^3 enclosure at Canadian Nuclear Laboratories (CNL) ([5], [6]) were used to validate a hydrogen release model developed in GOTHIC 8.2 [13], a general-purpose thermal-hydraulics code widely used for safety analysis of hydrogen transport and mixing behaviour. The size and shape of the enclosure were considered representative of single-vehicle residential parking garages. Given that the hydrogen risk in tunnels or underground garages can be different from residential garages because of their smaller height-to-length ratio and limited availability of natural ventilation, a $1/8^{th}$ scale model (3.3 m × 3.6 m × 0.7 m) of the maintenance garage examined by Ehrhart et al. [1] (referred to as "Sandia garage") was constructed for the present study. The purpose was to examine the light gas dispersion in an enclosure with the length-to-height ratio typical of parking garages. This paper compares GOTHIC simulation results with the experimental measurements conducted in the $1/8^{th}$ scale garage to assess GOTHIC's predictive capabilities. In addition, predictions from Lowesmith's engineering model [7] are also used to assess the capability of each approach to predict hydrogen dispersion in the garage.

2.0 EXPERIMENTAL METHOD

A 3D drawing of the experimental enclosure (3.07 m long, 3.36 m wide and 0.71 m high) is shown in Figure 1. The dimensions are scaled linearly from the Sandia garage. It is constructed from engineered extruded aluminium beams and polycarbonate sheets. It consists of six units; the adjacent units are connected along the beams by bolts with rubble seals between the connecting surfaces. The side-wall polycarbonate sheets are placed inside the slots of the beams with rubber seals along the edges. The ceiling polycarbonate sheets are bolted onto the beams along the perimeter of the units. Silicone sealant was applied to all the edges along the side walls and floor to minimize leakage. There are four air intake vents at the bottom of the side walls (labelled as BV – bottom vent, 0.17 m × 0.08 m each) and four exhaust vents at the ceiling (labelled as TV – top vent, 0.11 m × 0.11 m each). Under both natural and forced ventilation conditions, air enters from the bottom vents and light gas-air mixture exits from the top vents. A $1/8^{th}$ scale three-dimensional (3D) printed car was placed next to BV1 for the tests discussed in this paper.

To maintain a constant flow rate during the test, the helium injection was regulated by a Masterflex flow controller (MFLX32907-71). The controller has a measurement range of 0 to 10 SLPM with an accuracy of ±0.8% reading. Twenty-four XEN-5320 sensors were installed in the enclosure to measure helium concentrations (SPs in Fig. 1). The measurement accuracy was within ±0.2% helium by volume. The gas temperature and relative humidity (RH) inside the enclosure were measured at two heights using calibrated K-type thermocouples and Vaisala HMP 235 RH probes. The uncertainty of the thermocouples was ~2 °C to a 95% confidence level and the uncertainty of the RH probes was ±3% RH. Eight TSI air velocity transducers (model 8455-09) were mounted in the centre of each opening to measure the flow velocity through the openings. The measurement range is 0 to 5 m/s with an uncertainty ±2.0% of reading or ±0.5% of the full scale of the selected range.

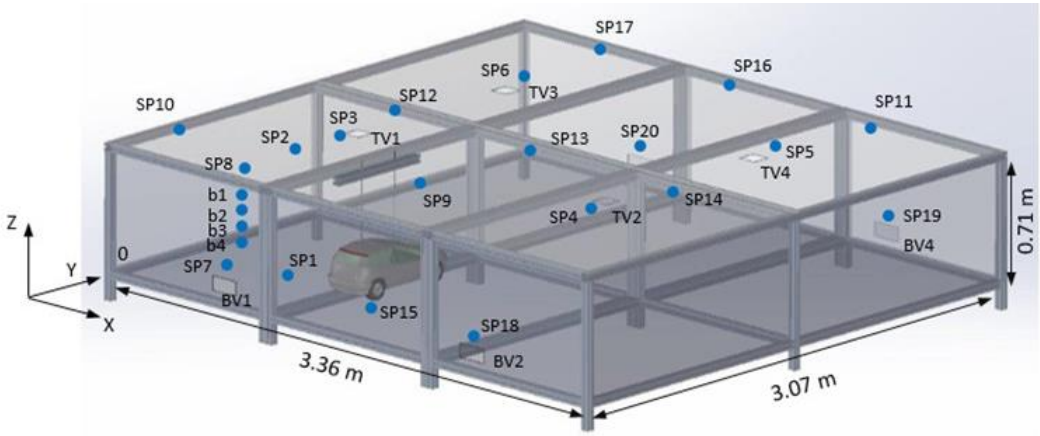

Figure 1. 3D drawing of scaled-down maintenance garage. The position of gas sensors (SP1-19 and b1-4) is indicated with blue circles.

In the Sandia study [1], a total of 2.5 kg of hydrogen was assumed to be leaking through a mid-pressure port (1.83 m above the ground) starting at 1.5 MPa. The leak diameter was assumed to be 0.86 mm. The resulting maximum release rate at the start of leak was 0.54 g/s and the tank was empty in approximately 210 minutes. The reference experimental conditions used in the present study were determined using the scaling relations developed by Hall and Walker [14]. The length and volume of the enclosure, injection rate, time and vent flow velocity are scaled by the relations of κ, κ^3, $\kappa^{5/2}$, $\kappa^{1/2}$ and $\kappa^{1/2}$, respectively, where κ equals to 1/8 here. A leak diameter of 1 mm was used in the tests, resulting in a lower injection velocity, but its impact on the far-field gas dispersion is not expected to be significant. Six tests are modelled using GOTHIC in this study. Their test conditions are summarised in Table 1. All the tests were performed under ambient conditions (1 atm, ~20°C and ~50% RH). The scaled-down release rate was 0.003 g/s (2.2 L/min), but a release rate of 1 to 10 L/min was used in this study. In the Sandia study, the release was relocated from 1.83 m to 0.61 m height. Both scaled-down heights were examined. In each test, helium was continuously injected through a downward-facing nozzle (1 mm diameter) below midpoint of the car at a constant rate until the helium profile reached a steady state. For test cases 5 and 6, an exhaust fan was placed on top of TV2 with a flow velocity of 1.0 m/s. The initial Reynolds number ($Re_0=\rho UD/\mu$) and Richardson number ($Ri_0=g(\rho_A-\rho_{He})D/(\rho U^2)$), for the conditions at the nozzle outlet are presented in In Table 1. In addition, the plume Reynolds number (Re_P) and Richardson number (Ri_P) were calculated assuming that the plume dimensions were in the order of magnitude of the car base; this assumption is reasonable from the plume characteristics shown in Figure 3 and 4. The Richardson number is indicative of the behaviour of the Helium flow with a 'jet-like' behaviour for low Ri (<<1) and plume like behaviour for larger values [15]. The Ri_0 and Ri_P in Table 1 suggests that at the nozzle, the helium flow is 'jet-like', but above the car the flow is 'plume-like'.

Table 1. Test matrix

Test Case #	Helium Injection		Forced Vent	Car elevation, base (m)	Reynolds Number (Re_0, Re_P)	Richardson Number (Ri_0, Ri_P)
	Rate (SLPM[1])	Elevation of Nozzle (m)				
1	1	0.06	No	0.110	400, 2.6,	1.90E-5, 2.35E8
2	5	0.06	No	0.110	2000, 13.0,	7.59E-7, 9.39E6
3	10	0.06	No	0.110	4000, 26.1	1.90E-7, 2.35E6
4	5	0.19	No	0.244	2000, 13.0	1.90E-5, 9.39E6
5	5	0.06	TV2	0.110	2000, 13.0	1.90E-5, 9.39E6
6	10	0.06	TV2	0.110	4000, 26.1	7.59E-7, 2.35E6

[1] Standard (air properties at 0°C, 1 bar) liters per minute

3.0 MODELLING METHOD

3.1 GOTHIC Model

The GOTHIC model layout and its nodalisation are shown in Figure 2. The experimental enclosure is represented by two control volumes, 2s and 3s; each is subdivided with a 3D Cartesian mesh. A finer mesh was used in the refined region (control volume 3s), where the car and helium injection nozzle were located, and a coarser mesh was used in the surrounding region (control volume 2s). The atmosphere surrounding the enclosure was modelled by a lumped parameter model (control volume 1). The grid nodalization is based on the grid sensitivity study presented in Section 4.1. The car and aluminum frames of the garage in the experimental setup were modelled using non-porous 3D blockages.

A boundary condition (1F) was used to model the helium injection, with the injection rate measured from experiments. The four top vents and four bottom vents were connected to the atmosphere using the flow paths (FPs). In the cases where forced ventilation was provided at the TV2 vent, a fan component was included along the flow path from the enclosure to the atmosphere, specifying the flow rate based on experimentally recorded values.

The FAVOR (Fractional Area/Volume Obstacle Representation) method was used to solve the governing equations of mass, momentum, and energy through the finite volume method. GOTHIC solves these equations on a fully rectangular grid, using a shifted grid for the momentum equation. The standard k–ε model was used to solve the turbulence kinetic energy and dissipation. The FAVOR method employs porosity functions in order to account for solid obstacles bounded in the rectangular mesh. The simulation used a first-order differencing scheme for both spatial and temporal derivatives. The adaptive time stepping method ensured that the Courant number remained below 1 and maintained the time step size below 0.5 s. The governing equations were solved through a conjugate gradient iterative technique using a first-order upwind semi-implicit scheme.

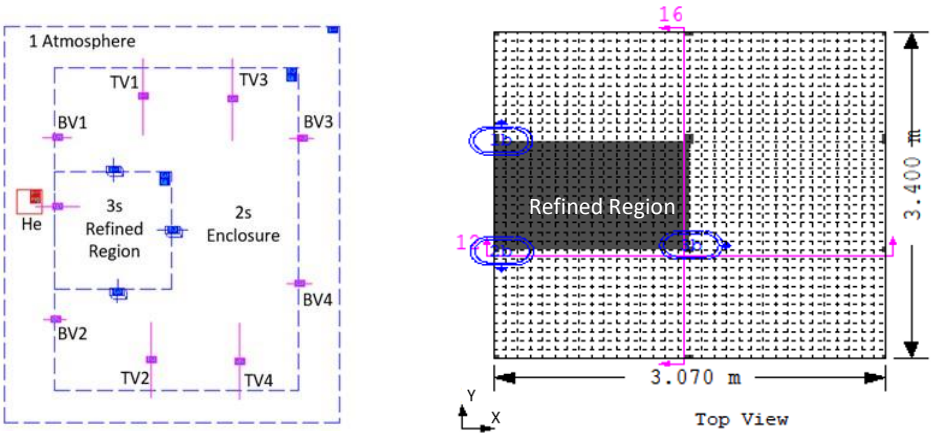

Figure 2. Layout of GOTHIC model (left) and subdivided control volume 2s for the main enclosure (right)

Table 2. Grid size

Control Volume	Region	Coordinate	Coarse	Medium	Fine
3s	Refined (car, injection)	Δx, m	0.055	0.043	0.035
		Δy, m	0.067	0.060	0.025
		Δz, m	0.034	0.028	0.021
2s	Enclosure	Δx, m	0.16	0.12	0.10
		Δy, m	0.12	0.10	0.08
		Δz, m	0.064	0.055	0.041

3.2 Engineering Models

As demonstrated in earlier studies [3- 8], when light gas is released into an empty enclosure filled with air, the light gas will rise as a vertical plume, reach the ceiling, spread to the sidewalls and descend in

the space between the sidewalls and the vertical plume. If the enclosure has openings at the top and bottom, the layer of buoyant fluid near the ceiling will drive an outflow through the top opening and an inflow through the lower opening. At the ceiling, a layer of light gas/air mixture will form, separated from the ambient air by a density interface. The depth of the buoyant upper layer will increase as the layer is fed with the light gas through the plume, and the interface will descend and approach the plume source. The analytical model developed by Lowesmith et al. [7] was used to predict the helium concentration in the upper uniform layer and the vent velocities for the natural ventilation cases as this model provided a better agreement with the experimental data than Prasad's model [8].

4.0 RESULTS AND DISCUSSION

4.1 GOTHIC Simulations: Grid Sensitivity

The mesh schemes provided in Table 2 were used to examine the grid sensitivity. Figure 3 shows the time histories of helium concentrations at two sensor locations (ceiling and floor) for Case 3. The helium concentration at SP10 (see Figure 1) was predicted reasonably well by the three predictions, but the helium concentration of the coarse mesh calculation contains strong oscillations at SP1 located on the floor. As SP1 is close to the injection nozzle and BV1 (Figure 1), the gas mixing and air entrainment could be over-predicted in the coarse mesh simulation, causing fluctuations at SP1. Overall, the fine mesh results demonstrate grid independence and these results are within the accuracy of the experimental sensors. Therefore, the fine mesh was used throughout this study.

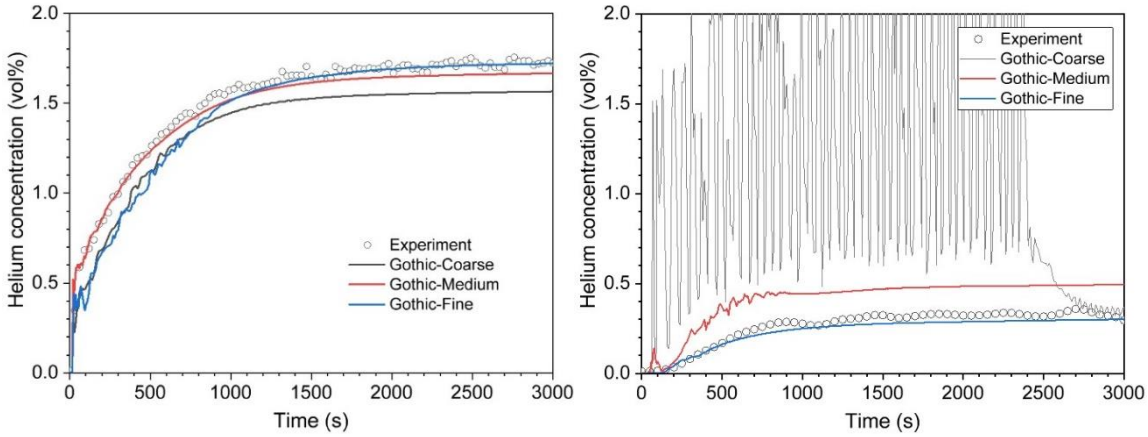

Figure 3. Time history of helium concentrations for case 3 (10 SLPM) at ceiling (SP10, left) and floor (SP1, right)

4.2 GOTHIC Simulations: Helium Concentration and Velocity Fields

The GOTHIC predictions of the helium volume fraction contours superimposed with velocity vectors for Case 2 (base case) are shown in Figure 4 to demonstrate the general behaviour of helium dispersion in the garage. In this test, the injection nozzle was located below the car at a height of 0.06 m and the injection rate was 5 SLPM. The vertical cross-sectional plane passes through the centre of the car. During the injection, the helium jet impinges on the floor and creates a recirculation region with high mixing below the car. The helium plume then moves around the car, entrains in the wake region above the car, then rises up, where it spreads across the ceiling. At 500 s, a layer of weakly stratified helium is formed near the ceiling, with the highest concentrations directly above the car. The upper layer of helium continues to grow as time progresses to 1000 s. Between 1000 s and 2500 s, the growth of the plume layer slows down, and the helium concentration in the garage reaches a steady state. This behaviour is consistent with the observation by Choi et al. [9].

The steady-state helium contours and velocity vectors for all six test cases are shown in Figure 5. At an injection rate of 1 SLPM and nozzle height of 0.06 m (Case 1), the downward helium jet does not reach the floor. The helium is nearly uniform in the enclosure at a fairly low concentration. A small amount of helium at a significantly higher concentration is trapped below the car, as observed by Ehrhart et al. [1]. Upon increasing the injection rate to 5 SLPM (Case 2), a significant amount of helium is trapped

below the car. The upper uniform layer extends to the mid-height of the car and exhausts from the garage at the top vents. When the injection rate is increased to 10 SLPM (Case 3), after the jet impinges on the floor, the helium spreads across the floor and rises up along the car vertical surfaces to the ceiling (nozzle is offset towards wall in the GOTHIC model because of the nodalization). The thickness of the upper layer is similar to Case 2, but the helium concentration in the upper layer is higher. When the car and injection nozzle were elevated to a height of 0.19 m (Case 4), the helium jet still reached the floor, but there was less interaction between the jet and the base of the car, and the mixing region was not observed around the car. The formation of the upper uniform layer remains similar to Case 2. In Case 5, a fan was placed at TV2, drawing gas at a velocity of 1.0 m/s. Similar to Case 2, a certain amount of helium is accumulated below the car, but the helium concentration in the upper layer is lower and the helium plume rise above the car is more prominent due to the enhanced ventilation. The forced-exhaust flow at TV2 also causes air inflow from other top vents. As a result, the helium layer is thinner, 'pushed-down' below TV1 due to the downward flow, and 'drawn-up' below TV2 due to the upward flow. At an injection rate of 10 SLPM (Case 6), the transport behaviour is similar to Case 3, but the helium concentration in the upper layer is significantly lower due to enhanced venting.

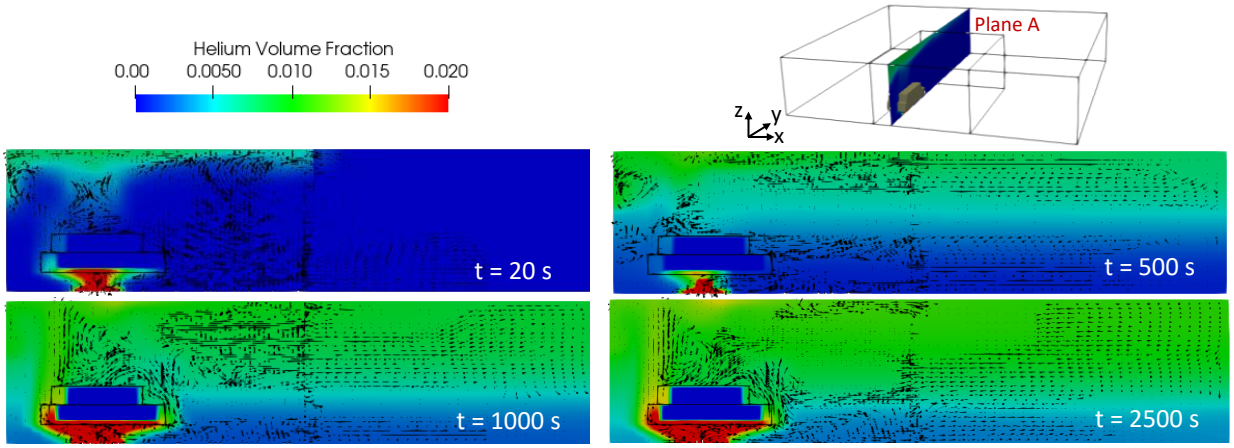

Figure 4. Helium volume fraction contours on vertical cross-section plane A at selected times for case 2 (5 SLPM)

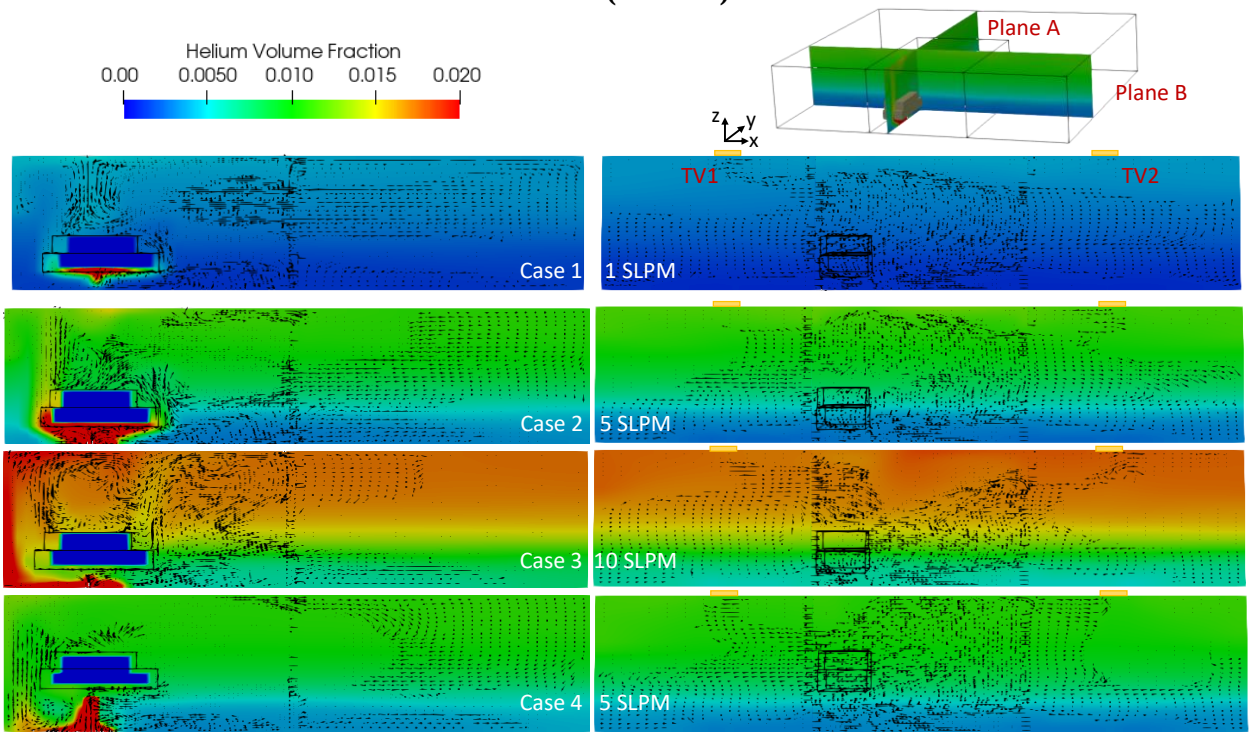

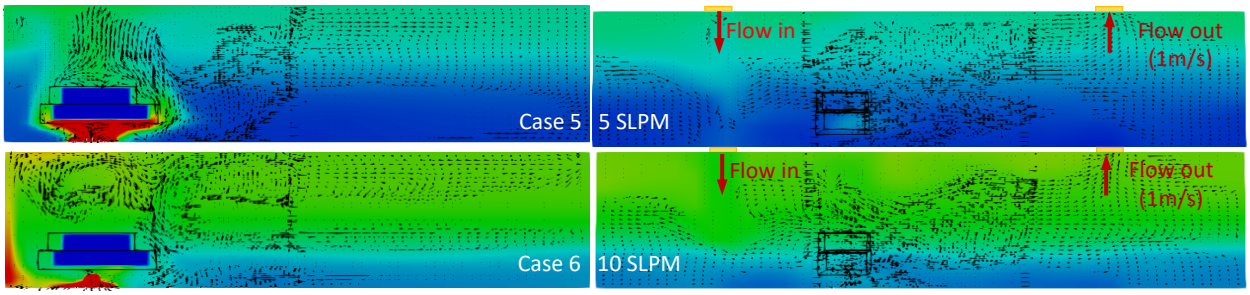

Figure 5. Steady-state helium volume fraction contours on two vertical cross-section planes (plane A: left column, plane B: right column) for Cases 1 to 6 (top to bottom)

4.3 GOTHIC vs. Experiments

Case 2 (Base Case): Helium Concentration and Vent Flow

Figure 6 compares the GOTHIC predictions for the helium concentration transients at the ceiling (left) and each vent (right) with the experimental data for Case 2 (base case). In both the experiment and simulation, the helium concentrations are not uniform across the ceiling. They are always slightly higher at the location above the car (SP9). The helium concentrations at TV1 and TV2 are always slightly higher than TV3 and TV4 as TV1 and TV2 are closer to the injection. The helium concentrations at the bottom vents are mostly the same, indicating that the helium front was relatively uniform across the horizontal plane when it moved downward. The GOTHIC prediction for the helium transients and the steady-state values are in close agreement with the experiments. At the bottom vents, GOTHIC slightly under-predicts the concentration. It should be noted that significant mixing occurred close to the bottom vents due to air entrainment. As a result, the GOTHIC predictions could vary greatly depending on minor variations in the sensor placement relative to the cell position in the mesh.

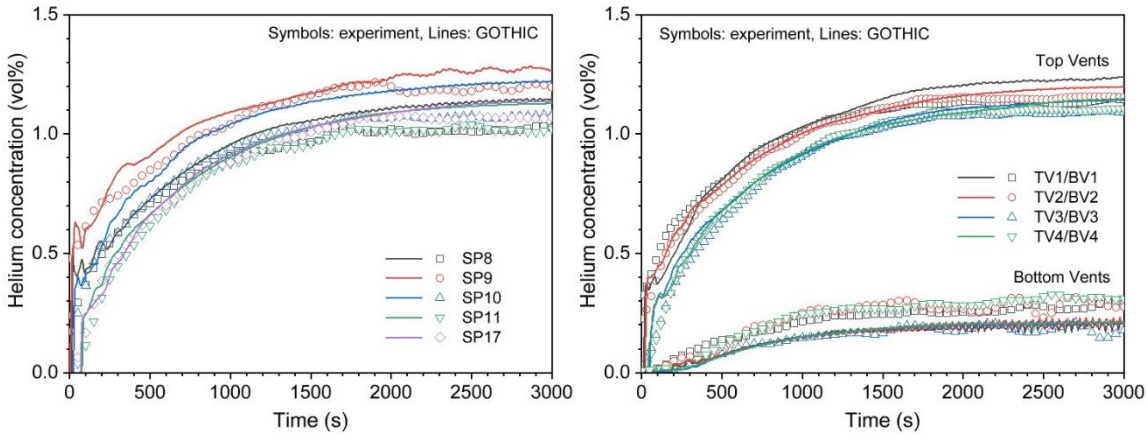

Figure 6. Time histories of helium concentrations at ceiling (left) and top and bottom vents (right) for Case 2 (5 SLPM, no fan, injection at 0.06 m height)

Figure 7 compares the GOTHIC prediction of vent flow velocity transients with the experimental data for Case 2. The velocity profile predicted by GOTHIC is the mean velocity at the vent. A hypothetical maximum velocity calculated using a multiplication factor of 1.5 (assuming a steady duct flow) is also presented in Figure 7 for comparison. It should be noted that the velocity sensor was placed at the center of each vent; therefore, the velocity measured in the experiments could be the highest value of the flow as the vent velocity can decrease from center to edge. In addition, the experiments show some deviations between vents; this could be attributed to two factors. First, the ambient flow surrounding the garage structure and around the vents was observed to have an effect on the vent flow in the experiments when the building ventilation was activated. Second, the test structure was not perfectly flat, leading to higher flow rates out of the vents where there was a greater accumulation of helium. Overall, the GOTHIC predictions at the top vents, multiplied by a factor of 1.5, show a better agreement with the experimental

measurements. The experimental data at the bottom vents are also bounded by the predicted mean velocity and hypothetical maximum velocity.

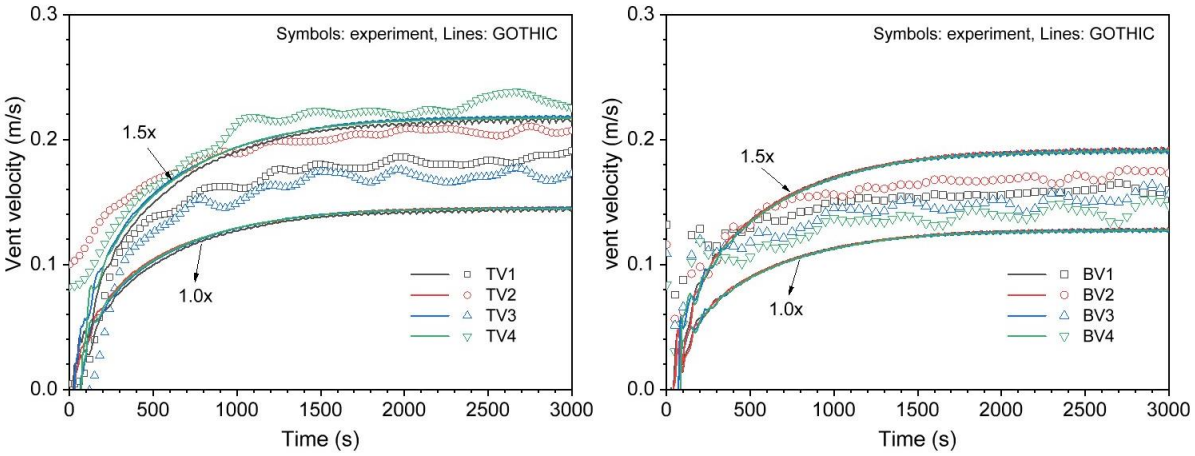

Figure 7. Time histories of vent flow velocities at top (left) and bottom vents (right) for Case 2

Effect of Injection Rate

Figure 8 (left) presents the relationship of time vs. projected radial distance (R) at different sensors on the ceiling for Case 3 during the initial spread of helium. The projected radial distance was the distance between each ceiling sensor and the origin of the injection nozzle projected on the ceiling. The time was determined based on when the helium concentration reached 0.15% at each sensor. In general, the sensor distance and time to reach 0.15% helium follow a linear relationship in the example of Case 3, but the data are more scattered at lower injection rates. The slope of the trend line is representative of the average spread rate of helium front across the ceiling. The spreading rate of the helium front predicted by GOTHIC is nearly identical to the measured spreading rate of 0.038 m/s for Case 3. The spreading rate becomes slower at a lower injection rate.

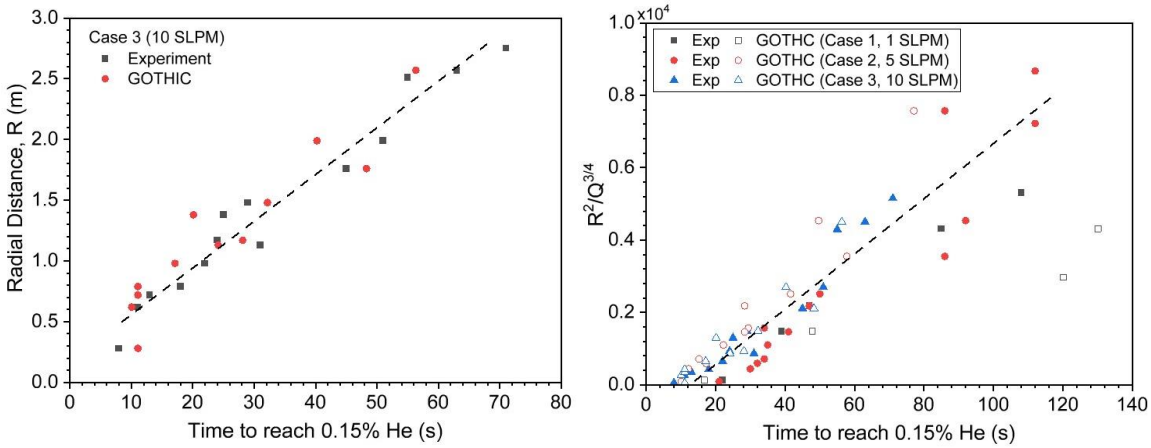

Figure 8. Distance vs. time for helium front spread across ceiling for Case 3 (left) and normalized distance vs. time for helium front spread for Cases 1, 2 and 3

Figure 8 (right) plots the normalized distance vs. time for Cases 1, 2 and 3. The normalized distance is expressed as $R^2/Q^{3/4}$, where R is in metres and Q is the injection rate in m^3/s. This normalization scheme was developed by Britter [166]. The author showed that the analysis was in agreement with the experimental results for the position of the leading edge of the plume advancing over a horizontal smooth surface. With this normalized scheme, the three sets of data collapse into one curve, especially within the initial 100 s. This suggests that the early horizontal spreading of the helium front was driven by the buoyancy and the spread rate was a function of the buoyancy flux emanating from the source, particularly during the initial spread. This finding is consistent with Xin et al. [11], who found that the initial release rate was the main factor in determining gas concentration distribution.

Figure 9 compares the GOTHIC predictions with the experimental data for the steady-state helium distribution along the height for Cases 1, 2 and 3. Experiment data corresponds to sensor positions in Figure 1 with SP data at 0.7 m and 0 m, BV data at 0.2 m, and b1 to b4 for data between 0.4 to 0.65 m elevation. The GOTHIC data were taken at three locations: the middle of the enclosure (through SP13), close to BV1, and far from the injection (through SP17). The GOTHIC data are generally not for the same location as the shown experimental data points, and could partially account for the deviations in the spatial distribution of helium in Figure 5. The simulations and experiments show that the vertical helium profile of Cases 2 (5 SLPM) and 3 (10 SLPM) consists of an upper uniform layer with a stratified layer at the bottom. The concentration decreases sharply below the 0.2 m height, where the bottom vents are located. The interface between the two layers is thinner at a lower injection rate. The upper layer almost disappears at the injection rate of 1 SLPM. The steady-state profile and the effect of the injection rate on the profile are the same as observed in the tests conducted in the enclosure with a larger height-to-length ratio [6]. Given that the experiment and GOTHIC data were not for the same *x*-*y* plane, the agreement for the steady-state profile between the simulations and the experiments is reasonably good.

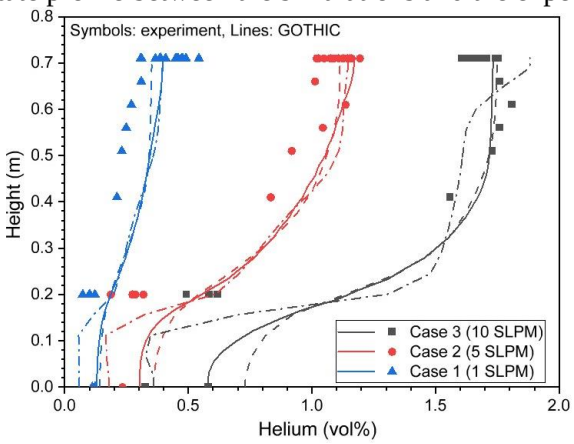

Figure 9. Comparison of vertical helium distribution for cases 1, 2 and 3. GOTHIC: vertical lines passing through SP13 (solid lines), SP17 (dash lines), and BV1 (dash-dot).

Effect of Injection Height

Figure 10 compares the time transients of helium concentrations between Cases 2 and 4. In Case 4, both the car and injector were at an elevated height of 0.19 m, while they were at 0.06 m in Case 2. In both the experiments and simulation, the overall helium concentration distributions are similar between the two cases except in the region close to the car. The helium concentration transients at the selected sensor locations are well captured in the simulation. The steady-state helium concentrations are slightly higher for Case 4 in the experiments, but GOTHIC predicts a lower steady-state helium concentration at SP9. The overall difference is within the measurement uncertainty. Nevertheless, both the experiments and simulations show that the effect of injection elevation on the bulk helium distribution is negligible between 0.06 m and 0.19 m.

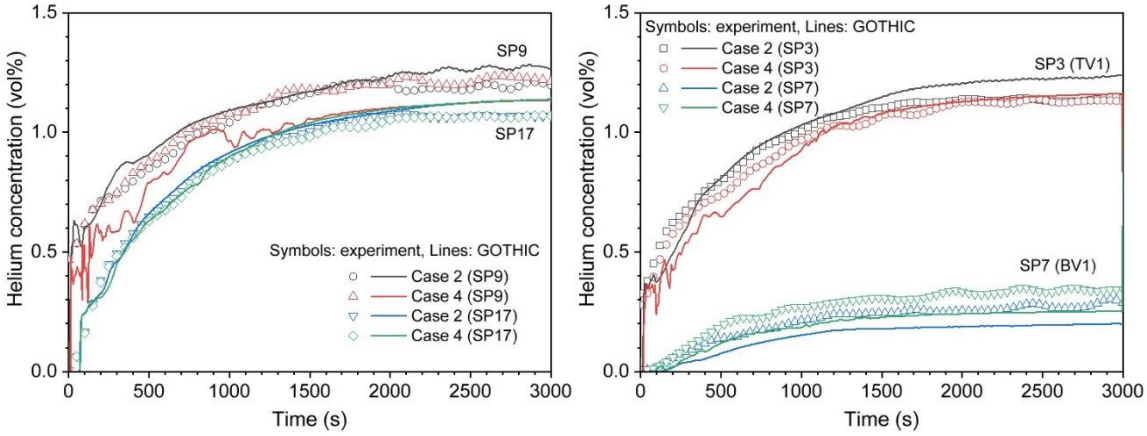

Figure 10. Comparison of Case 2 vs. Case 4 for helium concentrations at ceiling (left) and top and bottom vents (right)

Effect of Forced Vent Flow

Figure 11 compares the time transients of helium concentrations between Cases 2 (no active ventilation) and 5 (TV2 venting at 1 m/s). In the experiments, the flow velocities at the other top vents were nearly zero, meaning that the outflow only exited from TV2. In the simulation, air was pulled in from the other top vents at an average velocity of 0.13 m/s. The helium concentrations at all locations in Case 5 were significantly lower than Case 2. The results indicate that the use of a fan for venting had a noticeable effect in reducing the maximum helium concentration, but the impact is less effective with the fan applied only on one vent. The GOTHIC predictions at SP9 (above the car) and SP7 (BV1) match the experiment reasonably well, while they are under-predicted at SP17 (ceiling) and SP3 (TV1) for Case 5. The discrepancy could be attributed to the differences in velocity at the vents without the fan between the simulation and the experiment.

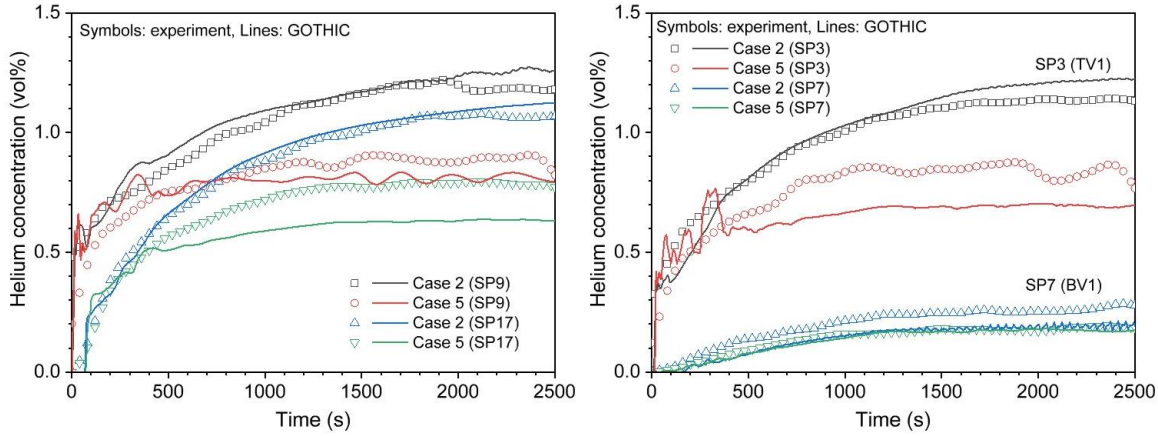

Figure 11. Comparison of Case 2 vs. Case 5 for helium concentrations at ceiling (left) and top and bottom vents (right)

4.4 GOTHIC and Lowesmith Model vs Experiments

Figure 12 compares the GOTHIC and Lowesmith's model predictions for helium concentration in the upper uniform layer and the vent flow velocities[2] with the experimental data for Case 2. The GOTHIC prediction for the helium concentration transient matches the experimental data well. The Lowesmith model slightly over-predicts the steady-state helium concentration and both vent velocities. The GOTHIC model also captures the trend of the vent velocities reasonably well. As discussed earlier, the discrepancy in the steady-state vent velocities was attributed to the fact that GOTHIC calculates the average value across the vent.

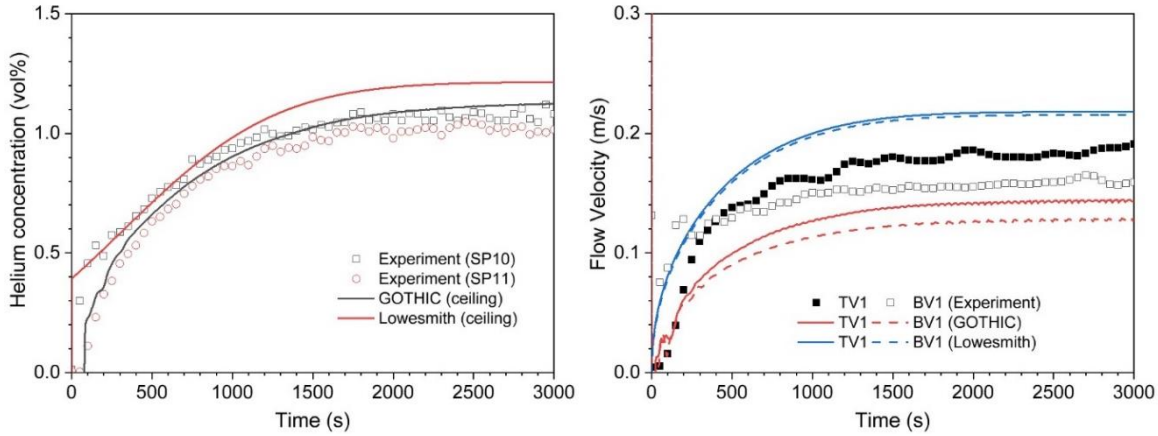

Figure 12. Comparison of GOTHIC simulation, experiments and Lowesmith model for Case 2: left for helium concentration at ceiling and right for vent velocities

[2] The experiment measured the centre velocity for the vent, whereas GOTHIC/Lowesmith are the average velocity.

The steady-state average helium concentrations at the ceiling sensors and flow velocities at both the passive top and bottom vents predicted by GOTHIC and Lowesmith's model for the six cases are compared with the experimental data in Figure 13. Lowesmith's model is not applicable for Cases 5 and 6, since it assumed natural ventilation, so only the predictions for Cases 1 to 4 are included. Under natural venting (Cases 1 to 4), the calculated helium concentrations and the vent velocities increase with the helium injection rate, which is in line with experiments. As discussed earlier, the discrepancy with the steady state helium concentration between GOTHIC and the experiment in Figure 13 was primarily attributed to three factors: (1) laterally varying vent velocity distribution and position of the sensor, (2) unevenness in the garage geometry that causes higher helium accumulation near some vents, and (3) variation of ambient conditions outside the garage vents would create differences in boundary conditions between vents. For Cases 5 and 6, the agreement between the GOTHIC predictions and experimental data for the helium concentrations remains good, but the discrepancy for the vent velocities is larger. Both the experiments and GOTHIC model need to be further investigated for the cases with ventilation.

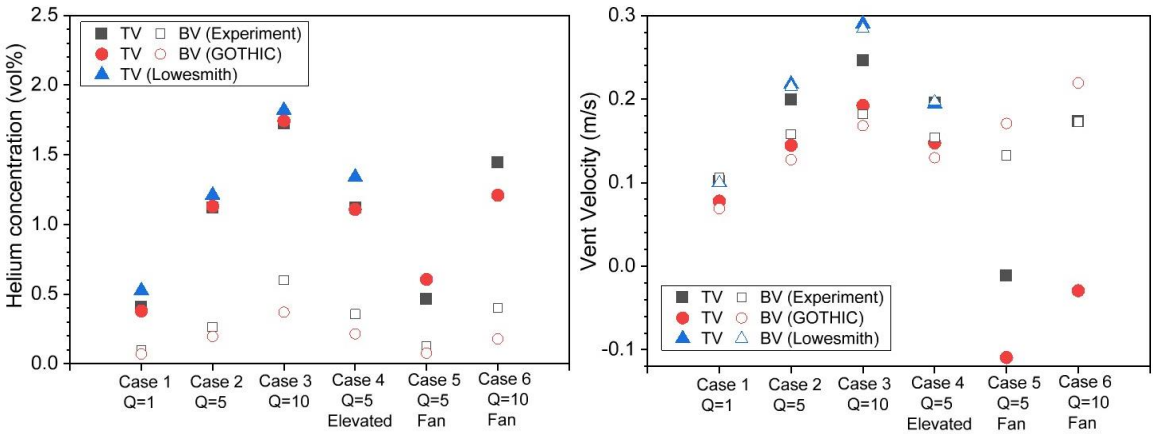

Figure 13. Comparison of steady-state ceiling average helium concentrations (left) and vent flow velocities (right) at top and bottom vents

5.0 SUMMARY AND CONCLUSIONS

This study examined the helium dispersion behaviour in a semi-confined enclosure (3.07 m long, 3.36 m wide and 0.71 m high), which represents a 1/8th scale maintenance parking garage for hydrogen fuel cell vehicles studied by the Sandia National Laboratories. Helium was continuously released through a downward-facing nozzle with a diameter of 1 mm below the model car until a steady-state was reached. The experiments showed that a steady-state helium profile and vent flow velocities were always reached during a continuous release. The helium was weakly stratified along the height at a lower injection rate, while at a higher injection rate, an upper uniform layer was always formed with a stratified layer at the bottom. The helium distribution was insensitive to the elevation of helium injection within the elevation range investigated. The position of the leading helium front during the initial spread was a function of the buoyancy flux emanating from the source.

Six tests were simulated using GOTHIC. Overall, GOTHIC demonstrated good predictive capability in capturing the transients of the helium distribution and vent flow. The simulations indicated that some helium accumulated underneath the car under both natural and forced ventilation conditions. The results from this investigation support the recommendation from the Sandia study [1] to use a local fan directed at the car during maintenance to prevent the potential accumulation of flammable gas near the car. In future studies the details of the hydrogen accumulation below the car will be evaluated using the GOTHIC simulations. Furthermore, the flammable envelope in the garage for each case will be characterized.

Lowesmith's model prediction for the helium concentration in the upper layer also matches the data reasonably well for the tests under natural convection. Overall, GOTHIC provides a good view of the local and global dispersion of helium in the garage. However, further refinement is necessary for both GOTHIC and analytical models to simulate cases with forced ventilation conditions, particularly regarding the induced flow at the passive vents.

ACKNOWLEDGEMENTS

The authors gratefully acknowledge the financial support from the Canadian Nuclear Safety Commission and Atomic Energy of Canada Limited, under the auspices of the Federal Nuclear Science and Technology Program.

REFERENCES

1. B.D. Ehrhart, S.R. Harris, L.L. Blaylock, A.B. Muna and S. Quong, Risk Assessment and Ventilation Modelling for Hydrogen Release in Vehicle Repair Garage, *Int J Hydrog Energy*, 46 (23), pp. 12429–12438, 2021.
2. S. Gupta, J. Brinster, E. Studer, and I. Tkatschenko, Hydrogen Related Risks within a Private Garage: Concentration Measurements in a Realistic Full Scale Experimental Facility, *Int J Hydrog Energy*, 34, pp. 5902–5911, 2009.
3. B. Cariteau, J. Brinster and I. Tkatschenko, Experiments on the Distribution of Concentration due to Buoyant Gas Low Flow Rate Release in an Enclosure, *Int J Hydrog Energy*, 36, pp. 2505 2512, 2011.
4. Houssin-Agbomson, D., Jallais, S., An Experimental Study Dictated to Wind influence on Helium Build-up and Concentration Distribution inside a 1-m3 Semi Confined Enclosure Considering Hydrogen Energy Applications Conditions of Use, 6th International Conference on Hydrogen Safety, 19–21 October 2015, Yokohama, Japan.
5. Z. Liang, A. McKenna, T. Clouthier, and R. David, Experimental Study on Accumulation of Helium Released into a Semi-Confined Enclosure with Distributed Leaks, *Int J Hydrog Energy*, 46, pp. 12522–12532, 2021.
6. Z. Liang, K. Barlow, and R. David, Experimental Study and Model Predictions on Helium Release in an Enclosure with Single or Multiple Vents, *Int J Hydrog Energy*, 91 (15), pp. 38884–38894, 2022.
7. B. Lowesmith, G. Hankinson, C. Spataru and M. Stobbart, Gas Build-Up in a Domestic Property Following Releases of Methane/Hydrogen Mixtures, *Int J Hydrog Energy*, 34 (14), pp. 5932–5939, 2009.
8. Prasad, K. and Yang, J.C., Vertical Release of Hydrogen in Partially Enclosed Compartment: Role of Wind and Buoyancy, *Int J Hydrogen Energy*, 36, pp. 1094-1106. 2011.
9. J. Choi, N. Hur, S. Kang, E.D. Lee and K.-B. Lee, "A CFD Simulation of Hydrogen Dispersion for the Hydrogen Leakage from a Fuel Cell Vehicle in an Underground Parking Garage", *Int J Hydrog Energy*, 38, pp. 8084 – 8091, 2013.
10. M.J. Chen, et. al, Measurements of Helium distributions in a Scaled-Down Parking Garage Model for Unintended Releases from a Fuel Cell Vehicle, *Int J Hydrog Energy*, 45(41), pp. 22166-22175, 2020.
11. J. Xin, Q. Duan, K. Jin, and J. Sun, A Reduced-Scale Experimental Study of Dispersion Characteristics of Hydrogen Leakage in an Underground Parking Garage, *Int J Hydrog Energy*, in press, 2023.
12. T. Huang, M. Zhao, Q. Ba, D. M. Christopher, and X. Li, Modeling of Hydrogen Dispersion from Hydrogen Fuel Cell Vehicles in an Underground Parking garage," *Int J Hydrog Energy*, 47 (1), pp. 686–696, 2022.
13. Voelsing, K., GOTHIC - Thermal Hydraulic Analysis Package Technical Manual Version 8.2 (QA), Electric Power Research Institute Inc., 2016 October.
14. D.J. Hall and S. Walker, Scaling rules for reduced-scale field releases of hydrogen fluoride, Journal of Hazardous Materials, volume 54, pp. 89 – 111, 1997
15. B. Cariteau and I. Tkatschenko, "Experimental study of the concentration build-up regimes in an enclosure without ventilation," Int J of Hydrg Energy, vol. 37, no. 22, pp. 17400–17408, Nov. 2012,
16. R. E. Britter, The Spread of a Negatively Buoyant Plume in a Calm Environment, *Atmospheric Environment*, Vol. 13, pp. 1241 – 1247, 1979